Scanning Microscopy Vol. 11, 1997 (Pages 241-250) 0891-7035/97$5.00+.25
Scanning Microscopy International, Chicago (AMF O'Hare), IL 60666 USA

ELEMENT SPECIFIC IMAGE ACQUISITION BY SAMPLING FOURIER COMPONENTS

B.M. Mertens* and P. Kruit

Department of Applied Physics, Faculty of Applied Sciences, Delft University of Technology, Delft, The Netherlands

Abstract

In electron microscopy, elemental information is usually acquired in real space by scanning a focussed probe over the specimen. We think there is a method to acquire elemental maps in Fourier space by sequentially sampling Fourier components.

The method is based on the illumination of the specimen with a pattern of fringes, a standing electron wave, and collecting, for instance, the X-ray spectrum as a function of fringe position, spacing and orientation. Each fringe spacing and orientation gives information about one Fourier component of the atomic distribution function for all elements in the specimen.

Image acquisition with this method has advantages over Scanning Transmission Electron Microscopy in terms of current and resolution. There is reason to believe that there are also advantages in terms of measurement precision, especially if the information sought for is highly localized in Fourier space.

Calculations show that the fringe scanning technique can lead to higher measurement precision, but only if the current in the standing wave illumination is higher than in the focussed probe. A resolution region is created where the answer to the question which of the two techniques gives a higher precision, depends on the number of Fourier components to be sampled and the required resolution.

Key Words: Analytical electron microscopy, super-resolution, electron holography, aperture synthesis, experimental design, measurement precision.

*Address for correspondence:
B.M. Mertens
TNO Institute of Applied Physics
Optics Division/Geometrical Optics
P.O. Box 155, 2600 AD Delft
The Netherlands

Telephone number: + 31 15 269 2417
FAX number: +31 15 269 2111
E-mail: mertens@tpd.tno.nl

Introduction

Elemental maps in electron microscopy can be acquired in a Scanning (Transmission) Electron Microscope (S(T)EM) by scanning a probe over the specimen. For dedicated STEM instruments, this technique can give elemental maps with resolutions slightly above 1A (Pennycook and Jesson, 1990), but for other instruments the limited probe size still prohibits resolving the atomic structure. The improvement of resolution is difficult as the ultimate probe size is determined by the wavelength of the electrons and the aberrations of the probe forming lens. Additionally, when the fundamental limit in probe size is approached, the achievable current in the probe reduces asymptotically to zero. This leads to extremely long measurement times and strong demands on instrument stability.

For certain material science questions there is a technique which gives elemental information at high resolution in a Transmission Electron Microscope (TEM), i.e., without the need to focus the beam to a small spot. This technique is called Atom Localization by Channeling Enhanced Microanalysis (ALCHEMI) (Spence and Taftø, 1983). It is based on the fact that the upper part of the specimen sets up an interference pattern by the dynamic diffraction process. By tilting the incoming beam over an appropriate range of angles, the interference maxima can be shifted over the different atomic sites in the lower part of the specimen. Information contained in the secondary signals, as a function of incoming beam tilt, can be used to differentiate between substitutional and interstitial atom site occupancy, even quantitatively (Spence and Taftø, 1983; Krishnan, 1988). The applicability of the technique is however limited as the specimen is both the object to set up the interference pattern and the object under study.

We think it should be possible to circumvent the disadvantages of STEM and ALCHEMI by using a fringe pattern (interference pattern or standing wave) to illuminate the specimen (Buist, 1995). By collecting a secondary signal, e.g., the X-ray fluorescence spectrum, as a function of the fringe position, spacing and orientation, the complete elemental map can be deduced as each fringe position and orientation gives information on one spatial frequency. The easiest way to see this is by giving an example (Fig. 1). In Figure 1a, a specimen is shown which consists of two atom

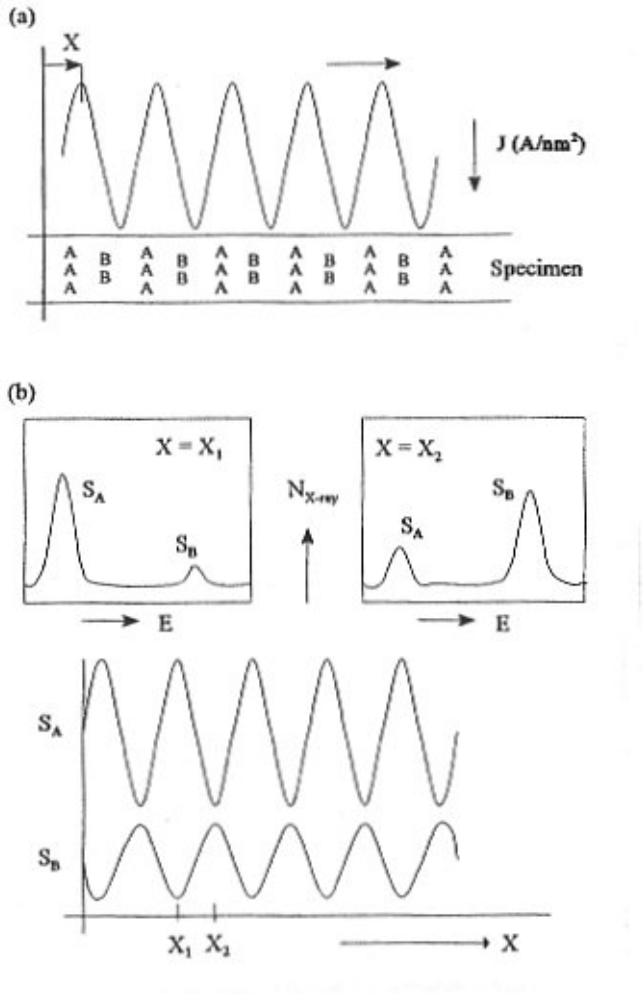

Figure 1. The principle of image acquisition with the fringe scanning method. The specimen is illuminated with a standing electron wave (**a**) and the X-ray fluorescence signal of atoms A and B is measured as a function of the position of the fringe pattern on the specimen (**b**).

types A and B. Both atom types have the same lattice spacing but the respective lattice planes have a different offset with respect to an arbitrary chosen origin and the atom types have different concentrations.

The specimen is illuminated with a fringe pattern with a periodicity equal to the lattice spacing and the X-ray spectrum is collected as a function of the position of the fringe maxima. The result is a periodic function (Fig. 1b), also with a spatial frequency equal to the lattice spacing. From the offset, or dc component, and the phase of this periodic signal, the concentration and the relative position of both atomic lattice planes can be determined. The relative amplitude of the periodic signal, A/I_0, and the phase can be related directly to the amplitude and phase of the Fourier component (of the atomic distribution function) corresponding to the fringe spacing.

In this example only one spatial frequency is used and it is therefore very simple: it is a typical ALCHEMI type of experiment. However, for more complicated crystals, many more fringe spacings (and also orientations) are needed to obtain the information on many different spatial frequencies. The possibility to measure information on many different spatial frequencies is the main advantage of the fringe scanning method over ALCHEMI. It gives the possibility, per element, to construct the Fourier transform of the atomic distribution function in the computer by conducting a sequence of ALCHEMI type of experiments. The calculation of the full elemental map in real space, after the measurements, involves only simple computer processing.

The advantage of the fringe scanning method over STEM is two-fold. Firstly, as the smallest possible fringe spacing at the specimen is below 1A, the resolution which can be obtained is higher. Secondly, if a beam splitter crystal is used, the obtainable current in the fringe pattern is larger than in a probe. This is because the fringes are imaged at the specimen with the two plane waves symmetrically through the imaging objective lens, so only the illumination opening angle in the plane wave determines the effect of the spherical and chromatical aberrations. It is similar to imaging a high resolution lattice structure in a TEM using only the scattered beams on the achromatic circle.

To make these arguments more quantitative the measurement of an elemental map with a given resolution and field of view is simulated, both for STEM and for the fringe scanning technique. In Figure 2, the current as a function of the resolution is depicted. It should be noted that information on the instrument for fringe scanning, which will schematically be described below, is included in the simulation.

An instrument to perform the fringe scanning measurement should be capable of creating the fringes and imaging them at the specimen with sufficient flexibility. What should this instrument look like? At first, a beam splitter needs to be positioned between the source and the specimen. The easiest way to do this is to insert an electrostatic biprism in the C2 aperture plane. This construction has disadvantages as the coherence width at the biprism level needs to be so large that no gain in current compared to STEM can be achieved. Also, there is little flexibility and the rotation of fringes using a rotatable biprism holder seems too difficult to do with sufficient reproducibility and accuracy. Therefore the use of a crystal beam splitter seems more appropriate. Inserting the crystal beam splitter in the C2 aperture is again not suitable as the objective has a strong demagnification and there is no flexibility in fringe distance. Also the possibility to put the crystal in the objective and the specimen in the selected

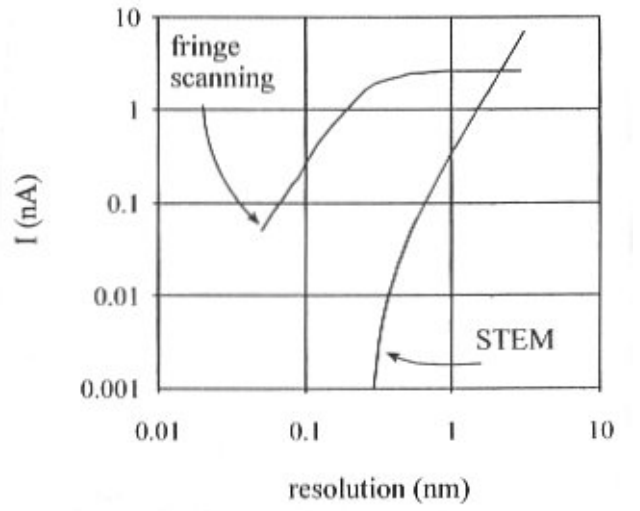

Figure 2. Simulation of the current as a function of resolution, both for STEM and for the fringe scanning technique. Values used in the calculations: brightness: $\beta = 2 \cdot 10^{12}$ A/(m^{2}Sr) at accelerating voltage U = 100kV; dU/U = 10^{-5}; $C_s = C_c = 2.0$ mm; beam splitter: Si (111) reflections; fringe visibility at the specimen level: V = 0.8.

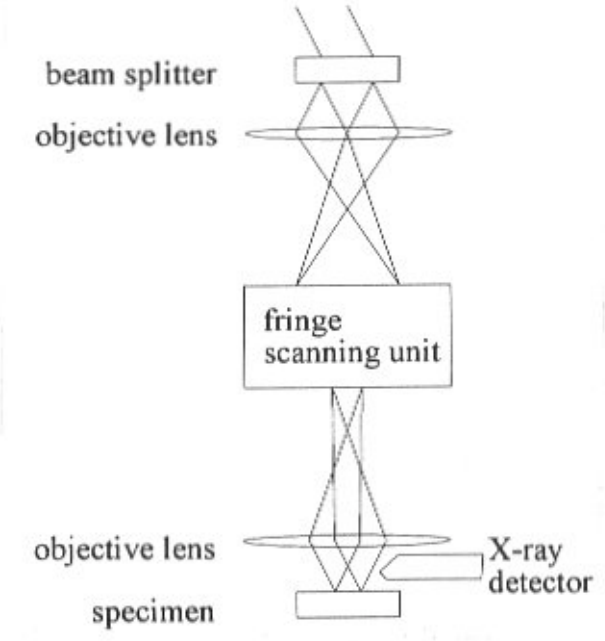

Figure 3. Schematic drawing of a part of the electron microscope for fringe scanning microscopy. Such a microscope needs, compared to a normal TEM microscope, an extension with an extra objective lens and some lenses for fringe magnification and rotation (i.e., the "fringe scanning unit").

area (SA)-aperture plane (Matteucci *et al*., 1981) leads to small flexibility in fringe formation and prohibits the formation of fringes with spacings in the sub-nanometer regime. Looking at the above arguments, it seems sensible to add an extra segment to the column with good imaging characteristics from the crystal beam splitter to the specimen. This means an extra objective lens and some magnetic electron lenses and deflectors between the two objectives for fringe magnification, rotation and shifting. In Figure 3, the optics are schematically depicted. The figure only shows the part of the column from the beam splitter to the specimen. The condenser system (with a field emission gun on top) and projector system to the camera are identical to a normal microscope.

At this point, assuming that only the aberrations of both objectives are relevant, the curve describing the current as a function of the resolution for the fringe scanning technique (Fig. 2) can be explained in a qualitative way. The curve shows two regimes: one where the current increases with decreasing resolution and one regime where the current is independent of the resolution. The behavior in the high resolution regime can be explained by realizing that there the fringe spacing at the specimen is smaller than at the beam splitter. Therefore, the specimen objective is limiting the acceptable illumination opening angle and this is identical to the situation where lattice fringes are imaged in a normal TEM. Then, also, as the spacing of the fringes decreases, the (aberration limited) illumination opening angle decreases for a given fringe contrast. In the low resolution regime the situation is reversed. Therefore, as the resolution is related to the fringe spacing at the specimen, going to lower resolutions does not increase the current as it will still be limited by the acceptable illumination opening angle (for a given fringe contrast) in the beam splitter objective.

Apart from the measurement procedure described above, other measurement procedures are possible based on the illumination of the specimen with a standing electron wave. Firstly, by illuminating the specimen with a large fringe spacing and imaging the exit fringe pattern on a CCD (charge-coupled device) camera with a certain defocus, an electron hologram with two unseparated images can be obtained. By the usual holographic reconstruction process, a differential phase contrast image can be obtained (Buist, 1995; Kruit and Buist, 1994). The technique is already applied to the investigation of magnetic films (Kruit *et al*., 1995; McCartney *et al*., 1996).

Secondly, the two plane waves both lead to diffraction patterns in the back focal plane of the objective which are only shifted with respect to each other. By adapting the tilt between the two incoming plane waves the diffraction patterns can be overlapped and due to interference effects

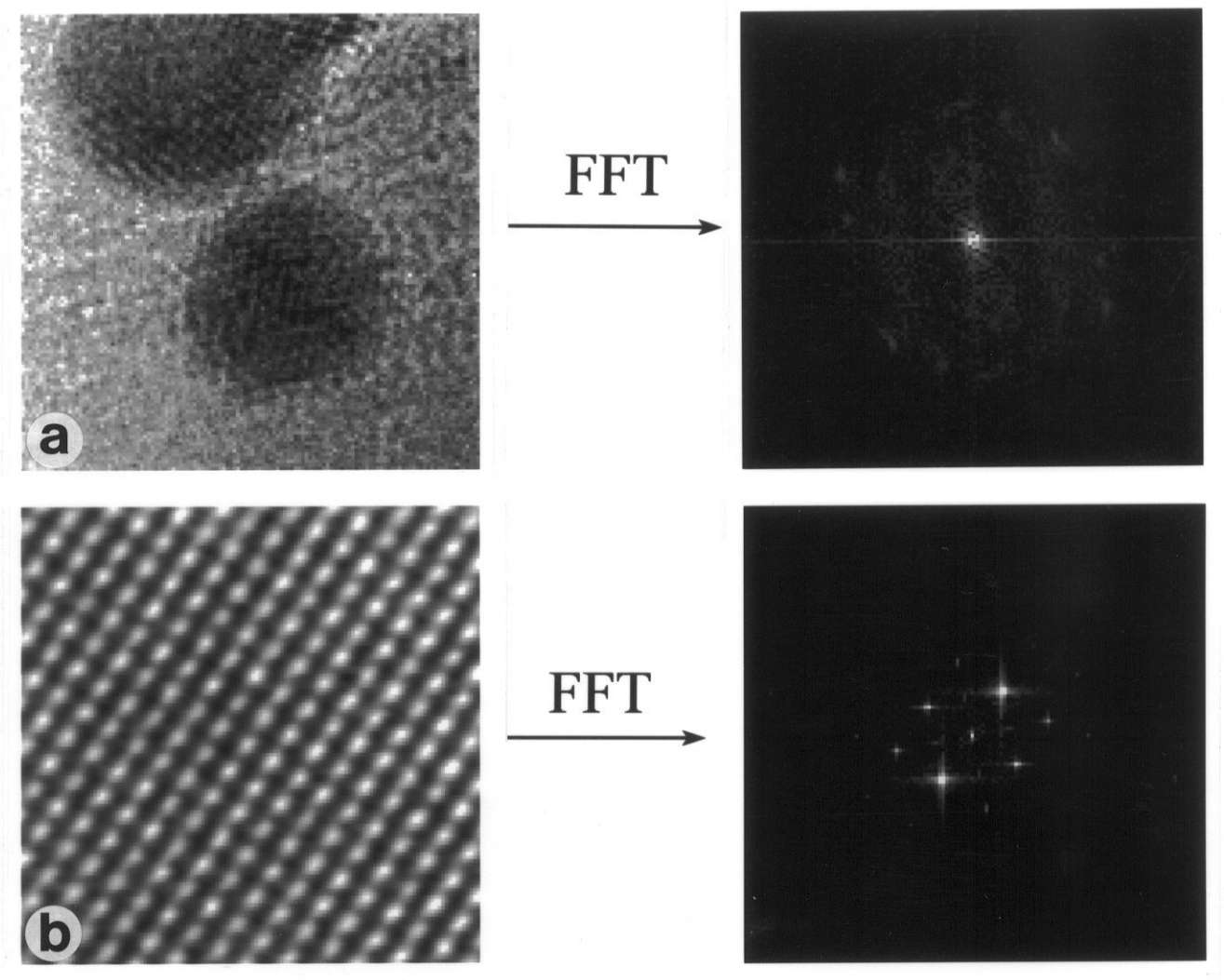

Figure 4. Measurements by sampling Fourier components as an additional possibility for intelligent experimental design. In the case of a non-periodic object (**a**) a measurement using S(T)EM seems better while in the case of a periodic structure (**b**), the fringe scanning method seems to be a logical choice.

in the overlap, the relative phases of the beams can be determined by observing the diffraction pattern intensity as a function of fringe position (Buist and Kruit, 1994). The technique is very similar to the principle of phasing in the diffraction plane as proposed earlier (Berndt and Doll, 1976; Kunath, 1978) and shows resemblance with the "ptychography" method as proposed by Hoppe (1969).

Possibilities in Experimental Design Using the Fringe Scanning Method

It seems reasonable to expect that the fringe scanning method, apart from the current and resolution advantages, might have additional advantages in terms of intelligent experimental design.

In high resolution STEM, the measurement precision is very low due to the low currents obtainable in the small spots. Therefore a very careful examination has to be conducted as to which type of measurement gives the most information on the parameters to be estimated. This process to find the best measurement is called intelligent experimental design and leads to an answer with the highest measurement precision in the parameters of interest. The new possibility to sample Fourier components individually also leads to the question whether new intelligent experimental designs are possible, or in other words, whether there are situations in which one would like to conduct the fringe scanning experiment in order to increase the measurement precision

in the parameters to be estimated.

Usually, before any low counting statistics experiment in the electron microscope is done, an experiment is conducted to find where the interesting features are. From this pilot experiment, a model of the object under study is developed and it is decided what the final experiment will be. For instance (Fig. 4a), suppose that from the pilot experiment, a TEM image, it shows that the object consists of small particles known to consist of atom A and B and the question to be answered might be: "are the particles made of a homogeneous alloy or is there a segregation with either atom A or B on the surface of the particle?". In this case it is best to zoom in on some particles and use all the available electrons to make line scans through the particles in a few directions. This is intelligent experimental design: choose the experiments which give most information on the parameters to be estimated.

In the same line of reasoning one can treat the example in Figure 4b. Here, the pilot experiment shows a periodic structure consisting of three types of atoms: A and B as matrix elements and C as an alloying component. The question might be typical for ALCHEMI type of experiments: "is atom C located at the position of A or B or is it slightly shifted from either of these positions?" In this case the information is in the phase of the Fourier components of the elemental map of atom C, relative to the phases of A and B. Therefore, in terms of intelligent experimental design, it seems logical to directly measure the phases of these Fourier components, i.e., using the fringe scanning method. The experiment can be performed by illuminating the specimen with the correct fringe spacing and looking at the number of X-ray counts as a function of the position of the fringe maxima. From the periodic signals, as in Figure 1b, the relative phases can be determined.

Concluding from the above example, it is expected that the possibility to perform fringe scanning experiments will lead to better experimental designs, at least in specific circumstances like ALCHEMI type of experiments. The question is now if we can prove this statement and make it more general. From the above example, it is expected that questions on periodic specimens lead to the choice to sample the Fourier components, while questions on non-periodic specimens lead to the choice to perform S(T)EM measurements.

Calculations

In order to get some idea whether or not new experimental designs are possible using the fringe scanning method, equations are derived for the relative precision of the dc component, the amplitude and the phase of a given Fourier component, both for STEM and for the fringe scanning technique. These equations will only be based on stochastic errors in the counting of the X-rays. In other words, it will be assumed that the machine is perfect.

For the fringe scanning experiment, the estimated parameters can be derived from measured intensities if the fringe shifting algorithm is known (Greivenkamp and Bruning, 1992). Here, the assumption of a perfect machine means that it is sufficient to do three intensity measurements to determine the amplitude and phase of a specific Fourier component, with the different fringe positions being exact.

The fringe shifting is used to measure the number of X-ray counts, I(x), as a function of the fringe position x, described by

$$I(x) = I_0 + A\cos\left(\frac{2\pi x}{d} + \phi\right) \tag{1}$$

where d is the fringe spacing, I_0 is the dc component, A is the amplitude and ϕ is the phase. As mentioned, the values for I_0, A and ϕ will be determined from three measurements I_1, I_2 and I_3. If the measurements are taken at the respective fringe positions x_1=-d/4, x_2=0 and x_3=d/4, the intensities are given by $I_1 = I(x_1)$, $I_2 = I(x_2)$ and $I_3 = I(x_3)$ and the values for I_0, A and ϕ can be found from:

$$I_0 = \frac{1}{2}(I_1 + I_3) \tag{2}$$

$$A = \frac{1}{2}\sqrt{2}\sqrt{(I_1 - I_2)^2 + (I_2 - I_3)^2} \tag{3}$$

$$\phi = \arctan\left(\frac{I_1 - I_3}{2I_2 - I_1 - I_3}\right) \tag{4}$$

From the uncertainty in the measured intensities due to the counting statistics, the relative uncertainties $\delta I_0/I_0$ in I_0 and $\delta A/A$ in A can be calculated:

$$\frac{\delta I_0}{I_0} = \frac{1}{\sqrt{I_1 + I_3}} \tag{5}$$

$$\frac{\delta A}{A} = \frac{\sqrt{(I_1 - I_2)^2 I_1 + (2I_2 - I_3 - I_1)^2 I_2 + (I_2 - I_3)^2 I_3}}{2A^2} \tag{6}$$

The absolute error $\delta\phi$ in ϕ is given by:

$$\delta\phi = \frac{\sqrt{(I_2 - I_3)^2 I_1 + (I_3 - I_1)^2 I_2 + (I_1 - I_2)^2 I_3}}{2A^2} \tag{7}$$

For STEM, the amplitudes and phases of the Fourier components can be estimated from the Fourier transform of the measured elemental map. The Fourier transform is a least squares estimator (Van den Bos, 1989) and the variance in the complex amplitude γ of any Fourier component, estimated from a Fourier transform, is given by (Smeets, 1995):

$$var(\gamma) = \frac{I_0}{N^2} \tag{8}$$

In Equation (8), I_0 is the dc component and N^2 is the total number of spot positions (in two dimensions) in the STEM experiment. From this variance the relative uncertainties in the dc component and the amplitude can be calculated:

$$\frac{\delta I_0}{I_0} = \sqrt{\frac{var(\gamma)}{I_0^2}} = \sqrt{\frac{1}{I_{tot}}} \tag{9}$$

$$\frac{\delta A}{A} = \sqrt{\frac{var(\gamma)}{A^2}} = \left(\frac{I_0}{A}\right)\sqrt{\frac{1}{I_{tot}}} \tag{10}$$

where I_{tot} is the total number of counts used in the experiment.

The absolute error $\delta\phi$ in the phase ϕ is:

$$\delta\phi = \frac{\delta A}{A} \tag{11}$$

The comparison will start with the situation where only the amplitude and phase of one Fourier component is estimated. Additionally, it is assumed that for both experiments an equal number of counts is used:

$$I_{tot} = I_1 + I_2 + I_3 \tag{12}$$

For the STEM experiment, the numerical values of the errors, given by Equations (9), (10) and (11), can be obtained directly by taking a Fourier transform of the measured elemental map and substituting the values, as calculated by the Fourier transform, for I_0 and A. The fringe scanning experiment can be simulated if the values for I_0, A and ϕ are used, together with Equation (12), to determine the expectation values for I_1, I_2 and I_3. These are then substituted into Equations (5), (6) and (7).

Both in STEM and in the fringe scanning technique, the formulas for the (relative) errors are inversely proportional to $\sqrt{I_{tot}}$. The number of counts can be eliminated by introducing the merit functions ξ, χ and ψ. The function ξ is defined by:

$$\xi = \frac{\left(\frac{\delta I_0}{I_0}\right)_{FS}}{\left(\frac{\delta I_0}{I_0}\right)_{STEM}} \tag{13}$$

where the subscript "FS" indicates the fringe scanning method. The merit functions χ and ψ can be obtained in a similar way by dividing Equation (6) with Equation (10) and Equation (7) with Equation (11) respectively. All these functions can be calculated analytically and appear to be dependent on A and ϕ. As an example, Figure 5 shows ξ as a function of ϕ for three values of A.

From Figure 5, it can be concluded that $\xi \geq 1$ for all possible values of A and ϕ. This conclusion also holds for χ and ψ. Therefore, for an equal number of counts, the fringe scanning method leads to less precise results compared to STEM, even for the estimation of the amplitude and phase of only one Fourier component.

The result can be explained as follows: for STEM, the noise is spread out in real space. Therefore, it is also spread out in Fourier space. The information on Fourier components, however, is very localized in Fourier space leading to a high precision; the estimation of amplitudes and phases of a Fourier component using the Fourier transform is ideal, so to speak. For the fringe scanning measurement, only three measurements contribute to the estimation of the amplitude and phase of a Fourier component. Therefore, the noise is also concentrated in these three measurements and the result for the fringe scanning measurement is less precise.

In a more general situation, the amplitudes and phases of more Fourier components need to be estimated, say M. Then, the results for all M components can be obtained simply by substituting the respective values for I_0 and A for each component as obtained by the Fourier transform. In other words, the precision for a given component is independent of the number of components.

In the fringe scanning experiment, more (i.e., M) fringe spacings and orientations are needed while for each spacing and orientation three measurements have to be done. Now the requirement for an equal number of total counts is:

$$I_{tot} = \sum_{m=1}^{M} (I_{1,m} + I_{2,m} + I_{3,m}) \tag{14}$$

where the subscript m denotes the m^{th} component. If, for instance, all counts are equally distributed over all Fourier components, then the sum of each of the measured intensities $I_{1,m}$, $I_{2,m}$ and $I_{3,m}$ for a given component m is equal to $I_{tot,m} = I_{tot}/M$. As the errors in Equations (5), (6) and (7) are inversely proportional to $\sqrt{I_{tot,m}}$, the merit functions are proportional to $\sqrt{M}$.

From the above arguments it should be concluded that, for an equal number of counts, the STEM measurement always leads to more precise estimates of the amplitudes and phases of Fourier components. However, as shown in Figure 2, the current in the fringe scanning technique can be substantially higher than in the STEM experiment. Therefore, the reduced measurement precision of the fringe scanning technique can be compensated by using a higher total number of counts. The balance between the reduced precision and the higher current can be

illustrated by plotting, in Figure 2, for the fringe scanning technique, the current divided by the average value of the merit function ξ (being equal to $\sqrt{(3 \cdot M/2)}$) (Fig. 6). In Figure 6, the microscope parameters are identical to the values used to calculate Figure 2.

From Figure 6 it can be seen that the lowest resolution where the fringe scanning technique is favorable over STEM becomes higher as the number of Fourier components increases. For instance, for one component, the trade-off is at about 2 nm while for 100 components, it is between 0.8 nm and 0.9 nm. Therefore, indeed, questions on periodic specimens make the fringe scanning technique more favorable and vice versa.

As successful many-beam simulations with in the order of 100 beams can be made for many material science applications (Voigt-Martin, 1995), one could say that for many material science questions with resolutions higher than 0.8 nm, the fringe scanning method is favorable in terms of measurement precision, while for resolutions lower than 2 nm, STEM is always favorable. In the resolution region between 0.8 nm and 2 nm, the actual decision which technique is favorable, is determined both by the required number of components for the question at hand and by the required resolution.

Conclusions

In this paper a method is presented to acquire images in Fourier space. The method is based on the illumination of a specimen with a standing electron wave, a fringe pattern. Information from secondary signals, e.g., an X-ray spectrum, as a function of the position of the fringes gives information on one Fourier component of the elemental map. By measuring all relevant Fourier components, i.e., performing a sequence of ALCHEMI type of experiments by applying all necessary fringe distances and orientations, a complete elemental map can be obtained.

The advantages of the fringe scanning technique compared to STEM are a higher obtainable resolution and current. The advantage compared to ALCHEMI is the flexibility in accessible Fourier components.

If an equal total number of counts is used for both techniques, for instance because of dose limitation, then there is no advantage compared to STEM in terms of measurement precision of estimated amplitudes and phases of Fourier components. This holds even for the situation where the amplitude and phase of only one Fourier component need to be estimated. If the amplitudes and phases of more Fourier components need to be estimated, the precision of the fringe scanning technique reduces proportional to $\sqrt{M}$ compared to STEM.

In situations where dose limitation is not an issue, the reduced precision of the fringe scanning technique can, in the high resolution regime, be compensated by the availability of a larger current. For many material science questions, a rough distinction between three resolution regimes can be made. For resolutions lower than 2 nm STEM is always favorable. In the resolution regime between 0.8 nm and 2 nm, the actual decision which technique is favorable in terms of measurement precision, is determined both by the required number of components for the question at hand and by the required resolution. For resolutions higher than 0.8 nm the fringe scanning technique is always favorable.

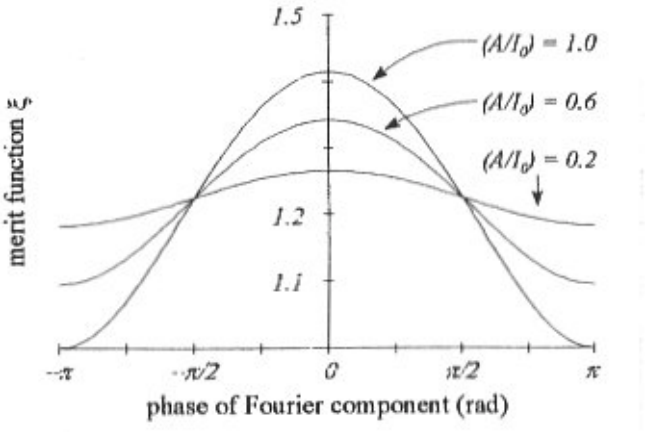

Figure 5: The merit function ξ as a function of the phase ϕ for different amplitudes A/I_0.

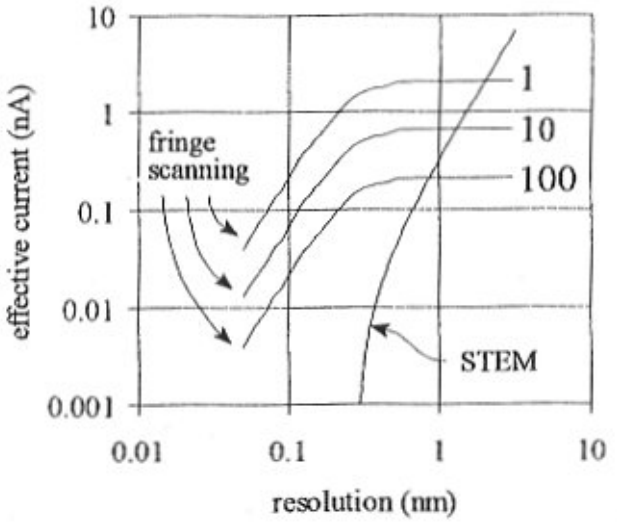

Figure 6: Calculated effective current of the fringe scanning method for three values of M, indicated in the top right corner, compared to the current in STEM. The effective current in the fringe scanning technique is the actual current divided by the average value of the merit function ξ (averaged over all values of the phase).

Acknowledgements

This work was sponsored by the Dutch Technology Foundation (STW) under project number DTN 33.2967.

References

Berndt H, Doll R (1976) Eine Methode zur direkten Phasenbestimmung in elektronenoptischen Beugungsbildern (A method for the direct phase determination of eplectron optical diffraction images). Optik **46**: 309-332.

Buist AH (1995) Information Extraction from Multiple TEM Images. Doctoral Thesis, Delft University of Technology, Chapter 3.

Buist AH, Kruit P (1994) Aplitude and phase measurements in TEM with electron standing wave illumination In: Proc 13th Int Congress Electron Microsc. Jouffrey B, Colliex C (eds). Les Editions de Physique, Les Ulis. Vol 1, pp 337-338.

Greivenkamp JE, Bruning JH (1992) Phase shifting interferometry. In: Optical Shop Testing. Malacara D (ed). John Wiley & Sons, Inc., New York. pp 501-598.

Hoppe W (1969) Beugung im Inhomogenen Primärstrahlenwellenfeld (Diffraction in an inhomogenous primary radiation wave field). Acta Cryst **A25**: 495-501.

Krishnan KM (1988) Atomic site and species determinations using channeling and related effects in analytical electron microscopy. Ultramicroscopy **24**: 125-142.

Kruit P, Buist AH (1994) Differential phase contrast in TEM. In: Proc 13th Int Congress Electron Microsc. Jouffrey B, Colliex C (eds). Les Editions de Physique, Les Ulis. Vol 1, pp 335-336.

Kruit P, Buist AH, McCartney MR, Scheinfein MR (1995) Differential phase contrast in TEM for magnetic microstructure observation. In: Microscopy and Microanalysis 1995. Bailey GW, Ellisman MH, Hennigar RA, Zaluzec NJ (eds). Jones and Begell Publishing, New York, pp 606-607.

Kunath W (1978) Phase determination from superposed diffraction patterns. Proc 9th Int Congress Electron Microsc, Toronto. Sturgess JM (ed). Microscopical Society of Canada, *city*. Vol 1, pp 556-557.

Matteucci G, Missiroli GF, Pozzi G (1981) Amplitude division electron interferometry. Ultramicroscopy **6**: 109-114.

McCartney MR, Kruit P, Buist AH, Scheinfein MR (1996) Differential phase contrast in TEM. Ultramicroscopy **65**: 179-186.

Pennycook SJ, Jesson DE (1990) High-resolution incoherent imaging of crystals. Phys Rev Lett **64**: 938-941.

Smeets RAM (1995) Schatten van Fouriercoefficienten uit Poissonwaarnemingen (Estimation of Fourier Coefficients from Poisson Observations). Master's Thesis, Delft University of Technology, Chapter 4.

Spence JHC, Taftø J (1983) ALCHEMI: a new technique for locating atoms in small crystals. J Microsc **130**: 147-154.

Van den Bos A (1989) Estimation of Fourier coefficients. IEEE Trans Instr Meas **38**: 1005-1007.

Voigt-Martin IG, Yan DH, Wortman R, Elich K (1995) The use of simulation methods to obtain the structure and conformation of 10-cyano-9,9′-bianthryl by electron diffraction and high resolution imaging. Ultramicroscopy **57**: 29-43.

Discussion with Reviewers

P.W. Hawkes: Please comment on the relation between this technique and Hoppe's "ptychography". There, structured illumination is recommended too, in that case in order to spread the diffraction spots out into overlapping discs.

Authors: Ptychography shows resemblance with the fringe scanning method where it is used to measure the amplitudes and phases of diffracted beams (Hoppe, 1969). In ptychography, coherent overlap between the diffracted spots is obtained by operating the microscope in STEM mode. Then, the diffraction spots broaden into discs and if the illumination opening angle is large enough and coherently filled, coherent overlap between adjacent diffraction discs occurs and the phases can be measured from the interference in the center of the overlap by shifting the probe.

There are three differences between ptychography and the fringe scanning method. Firstly, as the illumination has to be coherent over the full illumination opening angle, the obtainable current is much smaller than in the fringe scanning method. In fact, in ptychography, the coherence requirement leads to the same values for the current as in analytical STEM. Secondly, in ptychography, a full diffraction pattern is measured per probe position where, because many Fourier components are already present in the illumination, many Fourier components in the diffraction pattern determine the intensity profile in the center of the overlap as a function of the probe position. This might be a disadvantage in terms of necessary computing power to calculate the specimen exit wave, but can also be an advantage as it gives all information from only a few experiments. Thirdly, ptychography has no analytical equivalent to extend the resolution beyond the probe size, i.e., there is no way to build the elemental map from the measurement of amplitudes and phases of Fourier components, using some kind of secondary signal, e.g., X-rays. It is interesting to note that Hoppe, in his article, already proposed the fringe scanning method as an alternative for STEM ptychography for phasing of the diffracted beams.

P.A. Penczek: The analysis of the accuracy of the method presented in the paper is restricted to the error caused by the limited number of counts. The other source of error is an imperfect illuminating fringe pattern. Any deviations from a pure sine wave will limit the accuracy of the system. Was this effect considered, measured or estimated?
Authors: An imperfect illuminating fringe pattern leads to systematic errors in the estimation of amplitudes and phases of Fourier components, instead of stochastic errors. One can think about this as follows. The measurement of the periodic function as in figure 1b is in fact the measurement of the convolution of the object (or specimen) function with the illuminating function. In Fourier space this convolution is a product between the respective Fourier transforms. In the case of a pure sine wave, the Fourier transform of the illumination function has three Dirac delta functions: one at spatial frequency zero and two at spatial frequencies -q and q; the value of q is related to the fringe spacing. For pure sine wave illumination, the amplitude and phase of the convolution give the amplitude and phase of the Fourier component. For an imperfect fringe pattern, the Fourier transform of the illuminating function is broadened around the Dirac delta functions and the amplitude and the phase of the convolution, which are assigned to one Fourier component, are corrupted with information from other Fourier components.

An illuminating fringe pattern can be imperfect in two ways: the pattern can show a variation in fringe contrast over the field of view or it can show distortion, either radial or rotational. These forms of imperfectness are all related to the design of the microscope (including the beam splitter) and can therefore be minimized by a careful design. Contrast variations within the field of view are related to thickness variations in the beam splitting crystal, but also to an imperfect imaging system between the beam splitter and the specimen. Distortions are related to local crystal bending and also to an imperfect imaging system.

If, after minimization of contrast variations and distortions by careful design, there appear to be residual effects, then these can be dealt with by calibrating them. This can be done by doing measurements on more than three positions and including "coefficients of imperfectness" in the parameter estimation process.

N. Bonnet: Do you think that the Fourier space acquisition procedure is limited to elemental mapping or could it be generalized to other secondary signals?
Authors: The method is not restricted to elemental mapping with X-ray signals. In principle, other secondary signals are also possible, like EELS or Auger electrons.

S.J. Pennycook: The authors suggest that one of the potential advantages of the fringe illumination method compared to real space elemental mapping is access to higher Fourier components of the object. One approach that is very commonly employed in ion channeling studies is to take annular scans, that is profiles of direct scattering or secondary signals with high angular resolution. This is capable of providing positional information to a fraction of an Ångström. In electron channeling the same could be done, though interpretation of site information on a scale below that of the crystal planes would presumably require some dynamical diffraction calculations. However, would not such calculations also be needed if illuminating the specimen with fringes that were significantly below the planar spacing?

Although in this case one has the ability to vary the phase of the incident fringes with respect to the crystal planes, surely interpreting such results will still require a calculation of where the current is located inside the crystal?
P. Rez: The most serious conceptual problem with this paper is that the authors view electron intensity distributions inside a specimen as identical to the distribution on the entrance surface. I think they have been influenced too much by schematic pictures in the literature where various authors have tried to advertise their techniques by appealing to the notion of perfect channeling. In reality dynamical diffraction (and inelastic scattering) produces a "cross-talk" in real space. The correct procedure is to calculate the scattering of a wavefield representing the incident electron distribution using one of the standard computational techniques for dynamical diffraction. If one represents specimen scattering by a matrix operator (again computational method is unimportant) then it can clearly be seen that one incident Fourier component will generate all others:

$$\begin{pmatrix} \phi_0(t) \\ \phi_g(t) \\ \phi_{2g}(t) \\ . \end{pmatrix} = e^{(2\pi i)} \begin{pmatrix} 0 & \sigma & \sigma & . \\ \sigma & s_g & \sigma & . \\ \sigma & \sigma & s_{2g} & . \\ . & . & . & . \end{pmatrix} \begin{pmatrix} \phi_0(0) \\ \phi_g(0) \\ \phi_{2g}(0) \\ . \end{pmatrix} \quad (15)$$

D. van Dyck: The interaction of the electron probe with the X-ray generating object is described by the product of a probe function with an object function. How realistic is this approximation? What is the influence of dynamic scattering?
Authors: The question under what circumstances dynamical diffraction corrupts or maybe even destroys the measurement scheme as described in this paper, is equivalent to the question under what circumstances direct crystal interpretation from a reconstructed exit wave becomes impossible. Until recently, the assumption was that as long as the specimen could be considered a pure phase

object, direct interpretation was possible. In recent articles, the regime for direct crystal interpretation has been extended beyond the phase object approximation, at least under certain conditions for the accelerating voltage, crystal thickness and type of illumination (Van Dyck and Op de Beeck, 1996, Broeckx *et al*., 1995). The general conclusion from these articles is that for "most realistic HRTEM specimens" (thicknesses roughly around 10 nm) direct crystal interpretation is possible for accelerating voltages roughly between 100 kV and 300 kV. The form of the illumination function does play a role: the requirement is that the illumination function is smooth, i.e., the high frequency components in the illumination should be small. Although the regime for direct interpretation in case of standing wave illumination is not known, the conclusions from these articles provide hope that for fringe scanning also "most realistic high resolution TEM specimens" might be used.

In cases where direct interpretation is no longer possible, the calculation of the electron distribution in the specimen is indeed necessary and the technique becomes increasingly more difficult.

Additional References

Broeckx J, Op de Beeck M, Van Dyck D (1995) A useful approximation of the exit wave function in coherent STEM. Ultramicroscopy **60**: 71-80.

Van Dyck D, Op de Beeck M (1996) A simple intuitive theory for electron diffraction. Ultramicroscopy **64**: 99-107.